Dermatology Practical & Conceptual

Autoantibodies against Components of Sensory Nerve Formations in the Intervertebral Disks and Adjacent Structures are Antigens Recognized by the Sera from Patients Affected by a New Variant of Endemic Pemphigus in El Bagre, Colombia

Ana Maria Abreu Velez[1], Jorge Mario Vélez Arango[2], Yulieth Alexandra Upegui-Zapata[3], Adriana Milena Olarte Aponte[4], Melisa Naranjo Vanegas[5], Ivan Naranjo Vanegas[6], Jose A. Vega[7,8], Takashi Hashimoto[9], Michael S. Howard[1]

1 Georgia Dermatopathology Associates, Atlanta, Georgia, USA
2 Diagnostic Aids. Research Group on Images & AI in Health, SURA. Colombia, South America
3 Research Group in Infections and Health in the Tropics, School of Medicine, Universidad Nacional de Colombia, Bogota, Colombia, South America
4 Universidad Nacional de Colombia (National University of Colombia)
5 IQVIA Solutions Colombia S.A.S. Bogotá, Colombia
6 IPS SURA, Bogota, Colombia
7 Departamento de Morfología y Biología Celular, Grupo SINPOS, Universidad de Oviedo, Spain
8 Facultad de Ciencias de la Salud, Universidad Autónoma de Chile, Providencia- Santiago de Chile, Chile
9 Department of Dermatology, Graduate School of Medicine, Osaka Metropolitan University, Osaka, Japan

Key words: Endemic pemphigus foliaceus, Autoantibodies, Adjacent structures, Neural receptors

Citation: Abreu Velez AM, Vélez Arango JM, Upegui-Zapata YA, Olarte Aponte AM, Autoantibodies against Components of Sensory Nerve Formations in the Intervertebral Disks and Adjacent Structures are Antigens Recognized by the Sera from Patients Affected by a New Variant of Endemic Pemphigus in El Bagre, Colombia. *Dermatol Pract Concept*. 2025;15(4):5649. DOI: https://doi.org/10.5826/dpc.1504a5649

Accepted: June 12, 2025; **Published:** October 2025

Funding: Georgia Dermatopathology Associates, Atlanta, Georgia, USA, Mineros Colombia, Office of the major of El Bagre, Antioquia, Colombia South America, Japan International Cooperation, Colombia South America.

Competing Interests: None.

Authorship: All authors have contributed significantly to this publication.

Corresponding Author: Dr. Ana Maria Abreu Velez, M.D, Ph.D. DSc, Director of Research, Georgia Dermatopathology Associates, 1610 Lavista Road NE, Suite # 4, Atlanta, Georgia, USA. Phone 404-371-0077. Fax 404-634-5445. Email: abreuvelez@yahoo.com

ABSTRACT: **Background:** Patients affected by a new variant of endemic pemphigus foliaceus in El Bagre, Colombia have autoantibodies directed against different proteins in the skin and internal organs. In this study we investigated autoantibodies in the intervertebral disk (IVD) and surrounding spinal structures since most patients suffer from back pain.

Methods: We tested autoreactivity using indirect immunofluorescence, reflectance, and confocal microscopy using patient autoantibodies, with both human and bovine tissue as antigen sources. We tested 45 sera from patients and 45 control sera from the endemic area matched by age, sex, demographics, and work activity. Additional mass bone density and trabecular bone score (TBS) were determined in selected cases.

Results: Most of the patient sera revealed polyclonal autoreactivity against previously known and new neural receptors present in the IVD (translamellar cross-bridges of the annulus fibrosus and the nucleus pulposus), neurovascular bundles, and paraspinal neurovascular packages as well as in the anterior and posterior longitudinal ligaments ($P<0.001$). Patient autoantibodies co-localized with commercial antibodies to MYZAP, desmoplakins I–II, plakophilin-4, and ARVCF ($P<0.001$). Controls were negative. Triton X-100 and paraformaldehyde allowed us to see the complex morphological 3-dimensional shape of the nerves and receptors. We also found that the patients showed altered microarchitecture of the lumbar spine and low trabecular density, thus suggesting osteoporosis and/or osteopenia.

Conclusions: The autoantibodies to neural receptors in the IVD and surrounding structures and the osteopenia may contribute to patient back pain. Also, El Bagre-EPF autoantibodies provide a new tool to study the complexity of these neural receptors.

Introduction

An orphan autoimmune disease (a new variant of endemic pemphigus foliaceus, EPF; denominated pemphigus Abreu-Manu, or El Bagre-EPF) is present endemically in El Bagre, Colombia and surrounding municipalities and has been documented and partially characterized earlier [1-4]. In contrast to typical EPF, which primarily affects children and young adults, El Bagre-EPF affects older males and a few post-menopausal females [5]. Clinically, El Bagre-EPF is characterized by skin lesions; consistently, the primary autoantigens are cell junction proteins like plakins, i.e., desmoplakins, envoplakin, periplakin, and plakoglobin [6]. Other studies have demonstrated that El Bagre-EPF autoantigens were not restricted to cutaneous proteins but also proteins in internal organs [2-4]. In fact, using sera from those patients, Dr. Ana Maria Abreu Velez and co-workers discovered it contains autoantibodies against proteins that form parts of cell junctions and other membrane proteins as well as intracellular and nuclear proteins.

Patients affected by El Bagre-EPF frequently report back pain in the spinal area as well as low bone mass by densitometry, suggesting the involvement of spinal joints and ligaments, intervertebral disks (IVD), and, presumably, paraspinal muscles and fascia. Supporting this view, we detected autoantibodies against cells junction proteins in the IVD as well as in their surrounding structures (manuscript submitted). Whether additional nerves supplying all these structures are altered has never been investigated. Nonetheless, a reduction in cutaneous nerve fibers and fragmentation of the subepidermal neural plexus areas in El Bagre-EPF patients have previously been reported [7].

Therefore, our present research was designed to analyze in detail whether patients with El Bagre-EPF present changes in multiple anatomic structures of the lumbar region, including the peripheral nervous system.

Materials and Methods

As an antigen source, we bought fresh bovine vertebra including the intervertebral area from two- to three-year-old cows via a local United States Department of Agriculture (USDA)-certified slaughterhouse. Additionally, we used two lower IVDs from a human adult cadaveric tissue bank. Tissues were incubated for four minutes (min) with 1X PBS and 3.5% paraformaldehyde (to allow partial fixation, including lipids). We used this method to preserve some lipid components as well as Triton X-100 to expose membranes and intracellular antigens. Slides with tissue sections were then washed twice thoroughly with PBS for 10 minutes per wash and partly permeabilized using 1X PBS combined with 0.1% Triton X-100 (for partial solubilization of cell membranes and protein complexes) and 1% normal goat serum (for blocking). For our complete methods, please see File S1, and Table 1.

Further, in El Bagre-EPF patients and the correlated controls, spine densitometry was evaluated via an osteodensitometry analysis using Prodigy DXA systems© 2024 GE HealthCare™. GE Healthcare (Chicago, Illinois, USA)

Table 1. Antibodies Used for the IIF and Confocal Microscopy Studies, their Dilutions, Catalog Numbers, and Sources. We also present the commercial antibodies that colocalize with the commercial autoantibodies.

Catalogue No.	Antibody description, dilution, and producer. Dilute all in PBS IX. Dil=Dilution		
SKU:114202	Anti-human albumin FITC, High F/P - 5-9.0, Dil 1:50, From Kent Laboratories (with sodium azide 0.1%).		
SKU 104202	Anti-human IgE FITC 1:25 Dil, Low F/P - 2-4.9, from Kent Laboratories.		
SKU:117202	Anti-human Kappa FITC, Low F/P - 2-4.9, Dil 1:50 from Kent laboratories.		
SKU:110202	Anti-human complement C-5 (B1F) FITC, Low F/P - 2-4.9, Dil 1:25, from Kent laboratories		
SKU 103202	Anti-human IgM FITC (mu chain specific), Low F/P - 2-4.9, Dil: 1:25, from Kent laboratories.		
SKU:105202	Anti-human complement C-3 (B1C/B1A) FITC, Low F/P - 2-4.9, Dil 1:25, from Kent laboratories.		
SKU:116202	Anti-human immunoglobulins (IgA, IgA, IgM) "Polyvalent" FITC, Low F/P - 2-4.9, Dil 1:25, from Kent laboratories.		
SKU:111202	Anti-human C1q FITC, Low F/P - 2-4.9, Dil 1:20, from Kent laboratories.		
SKU:101202	Anti-human IgG FITC, Low F/P - 2-4.9, Dil:1:25, from Kent laboratories.		
SKU: CON-102202	Anti-human IgA FITC, Low F/P - 2-4.9, Dil:120, from Kent laboratories.		
SKU:127202	Anti-human IgD FITC, Low F/P - 2-4.9, Dil: 120, from Kent laboratories.		
SKU: 109202	Anti-human complement C-4 (B1E) FITC, High F/P - 5-9.0, Dil: 120, from Kent laboratories.		
SKU: 107202	Anti-human fibrinogen FITC, Low F/P - 2-4.9, Dil 1:50, from Kent laboratories.		
SKU: 118242	Anti-human lambda FITC, Dil 1:25, from Kent laboratories		
GP155, Progen, Germany	Polyclonal antibody to ARCVF source guinea tested in human and bovine (100ul).	A31570, Invitrogen	Alexa fluor® 555 goat anti-guinea pig (H+L) highly cross-adsorbed from Molecular Probes Life technologies, Invitrogen, ThermoFisher.
65146 Progen	Mouse monoclonal multi-epitope cocktail to anti-desmoplakin 1 & 2, (reacts with human, bovine, dog, rat, mouse chicken) (5ml vial). Clones DP-2.15, DP2.17, DP-2.20.	Goat anti-mouse Texas red conjugated IgG (H & L).	Catalog # T-6390 from Molecular Probes Life technologies, Invitrogen, ThermoFisher Scientific.
641166 Progen	Mouse monoclonal multi-epitope cocktail to -anti-P0071 (reacts with human, bovine, murine) (5ml vial). Clones 406.3.1, 433.10.3, 7.7.9.	Goat anti-mouse Texas red conjugated IgG (H & L).	Catalog # T-6390 from Molecular Probes Life technologies, Invitrogen, ThermoFisher Scientific.
651169 Progen	Mouse Mab to Myozap. Clone 517.67	Goat anti-mouse Texas red conjugated IgG (H & L).	Catalog # T-6390 from Molecular Probes Life technologies, Invitrogen, ThermoFisher Scientific

Osteodensitometry includes testing bone mineral density (BMD) to search for osteoporosis as well as an Optional Integrated Trabecular Bone Score (TBS). An Advanced Hip Assessment (FRAX)® was used to assess borderline cases. The dual absorption of X-rays were performed via General Electric Prodigy advance. We also reviewed axial slices of the spines using a Philips Brilliance *CT 16-slice* computerized tomography (CT) (CT16) scanner© Koninklijke Philips N.V.USA), with multiplanar coronal and sagittal reconstructions.

Results

The CT16 scans available in five patients and in five controls indicated no observable fracture trace in the bone window cuts. However, the presence of osteophytes (also called bone spurs) in lumbar vertebral bodies were seen in El Bagre-EPF patients and not in the controls. Furthermore, specific alterations in bone densitometry were detected at the lumbar spine scan. In L1–L4, a bone mass density (BMD) of 0.923 g/cm2, equivalent to a T-SCORE -2.1, was demonstrated. In the dual hip scan femoral neck, a BMD of 0.751 g/cm2 was equivalent to a T-SCORE. -2.1, and a Z-SCORE of -1.5. In the hip total scan, a BMD of 0.822 g/cm2 was equivalent to a T-SCORE -1.5 and a Z-SCORE of -1.2. These results indicated low bone mass by densitometry. It was suggested to rule out secondary causes via TBS: 1,228 partially deteriorated microarchitecture points (Figure 1). As far as we know, no bone change has ever been reported in Bagre-EPF patients.

In Figure 2 we summarize the results for the positivity found against multiple proteins located in the IVDs and their surrounding structures. All 45 patients affected by the El Bagre-EPF (combining the Senear-Usher-like and systemic disease forms) displayed autoantibodies against multiple proteins detected in the anterior and posterior longitudinal ligaments, in the annulus fibrosus (AF), and in the nucleus pulposus (NP). The same proteins, in variable amounts, were also detected in sensory nerve formations (SNFs) of different shapes and sizes present in the paraspinal structures and the neurovascular branches feeding and innervating these structures. The autoimmune response against all SNFs was polyclonal in nature. None of the controls from the endemic area showed positivity against these structures. Most of the SNFs identified do not correspond with typical morphotypes of SNFs reported in the IVD and paraspinal structures.

In figure 3, we show examples of multiple positive sensory nerve formations (SNFs) and the neural receptors at the fibrosus (AF) and in the nucleus pulposus (NP) as part

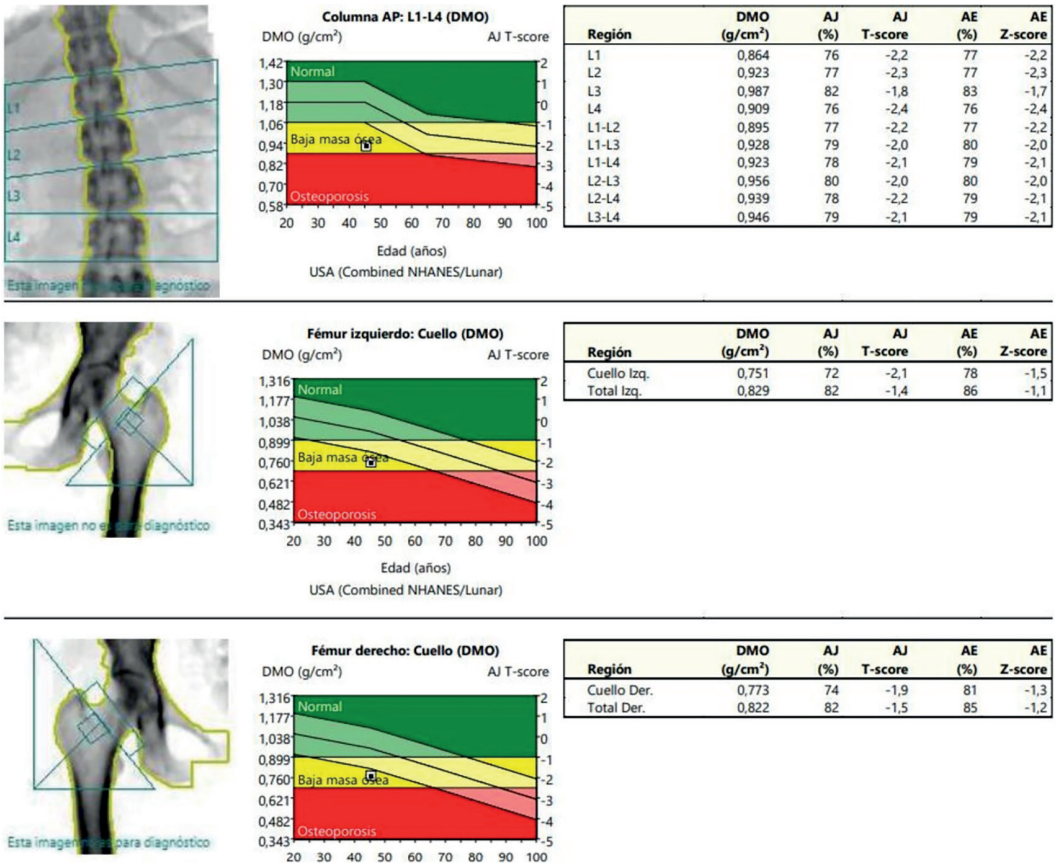

Región	DMO (g/cm²)	AJ (%)	AJ T-score	AE (%)	AE Z-score
L1	0,864	76	-2,2	77	-2,2
L2	0,923	77	-2,3	77	-2,3
L3	0,987	82	-1,8	83	-1,7
L4	0,909	76	-2,4	76	-2,4
L1-L2	0,895	77	-2,2	77	-2,2
L1-L3	0,928	79	-2,0	80	-2,0
L1-L4	0,923	78	-2,1	79	-2,1
L2-L3	0,956	80	-2,0	80	-2,0
L2-L4	0,939	78	-2,2	79	-2,1
L3-L4	0,946	79	-2,1	79	-2,1

Región	DMO (g/cm²)	AJ (%)	AJ T-score	AE (%)	AE Z-score
Cuello Izq.	0,751	72	-2,1	78	-1,5
Total Izq.	0,829	82	-1,4	86	-1,1

Región	DMO (g/cm²)	AJ (%)	AJ T-score	AE (%)	AE Z-score
Cuello Der.	0,773	74	-1,9	81	-1,3
Total Der.	0,822	82	-1,5	85	-1,2

Figure 1. Shown are the body mass density (BMD), the Trabecular Bone Score (TBS), and the computerized tomo graphy studies on one of the El Bagre-EPF patients.

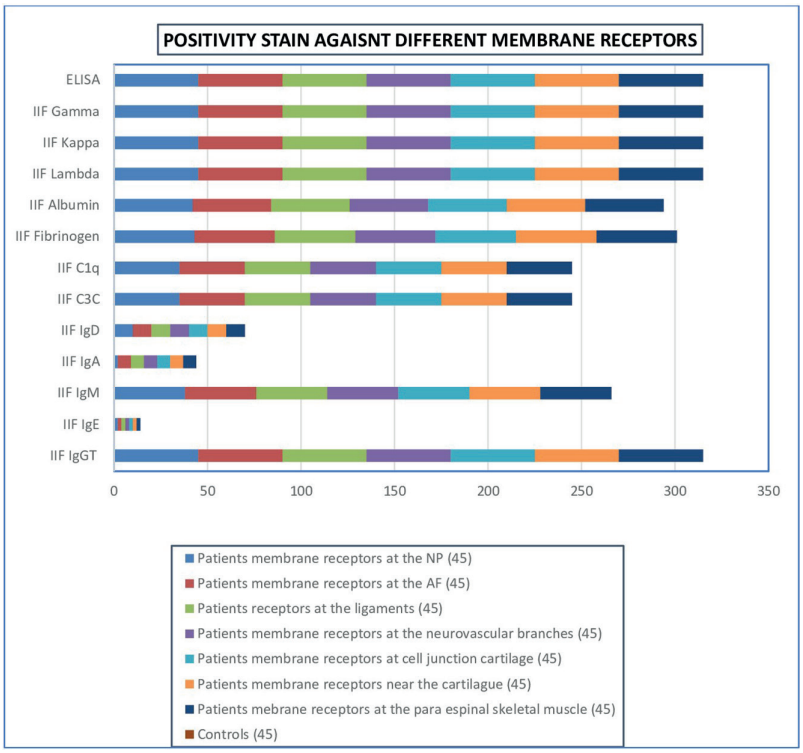

Figure 2. Summary of the results for the positivity found against multiple proteins located in the IVDs and their surrounding structures comparing patients and controls.

of the intervertebral structures. Most (43/45) of the patient sera exposed polyclonal autoreactivity with the antibodies against human (IgG, IgM, IgD, Kappa, Gamma, C3C, C1Q, and C4), (P<0.001) as well as positive with antibodies against fibrinogen and albumin against previously known and new neural receptors present in the IVD (translamellar cross-bridges of the annulus fibrosus, and the nucleus pulposus), neurovascular bundles, paraspinal neurovascular packages, and the anterior and posterior longitudinal ligaments. Controls were negative (P<0.001). In figure 4, we confirm by confocal microscopy the positivity and 100% colocalization of the patients autoantibodies with the commercial antibodies to plakophilin 4 (p0071), armadillo repeat gene deleted in the velo-cardio-facial syndrome (ARVCF), desmoplakins I and II (DP I-II), and myocardium-enriched zonula occludens-1-associated protein (MYZAP) (P<0.001). Several of the SNFs did not show the morphology of the currently documented sensory corpuscles in connective tissues, including IVD and paraspinal structures. Of interest, the neural receptors were of different forms and shapes, with some large globular structures and some smaller, and some along the myelinated fibers presenting as thinly encapsulated clusters.

Discussion

We recently demonstrated that El Bagre-EPF displays autoreactivity against proteins in tissues of the intervertebral disk (IVD) and adjacent structures with anomalies in the spine and using radiographs and magnetic resonance imaging (MRI) and the Back Pain Functional Scale (BPFS). Here we extended the focus to the cartilage of the IVD, the bodies of the lumbar vertebrae, and the paraspinal ligaments and muscles, since patients who suffer from El Bagre-EPF disease frequently report lower back pain. In the current study, lumbar osteophytes with decreased bone density were observed in some El Bagre-EPF patients relative to the controls. Whether these bone and joint alterations are a result of the El Bagre-EPF disease remains to be established, because pertinent diagnostic equipment is not available in the endemic area and thus not all the patients and controls have access to this.

In the present study, the most interesting finding was that in El Bagre-EPF patients there was great involvement of presumably afferent nerve fibers and SNFs, present both in intervertebral discs and in tissues surrounding them. We also confirmed that both the neurovascular bundles in the IVDs and surrounding structures had multiple SNFs recognized as antigenic in patients affected by El Bagre-EPF. Interestingly, these membrane receptors also perfectly colocalized with multiple commercial antibodies including DPI-I, MYZAP, p0071, and ARVCF. The MYZAP ARVCF, DP-I II, and p0071 are autoantigens detected by El Bagre-EPF patient sera, especially of those who have clinical forms resembling Senear-Usher syndrome and the systemic form that affects cell junctions throughout the body. We previously described that the patient sera contained autoantibodies against classic

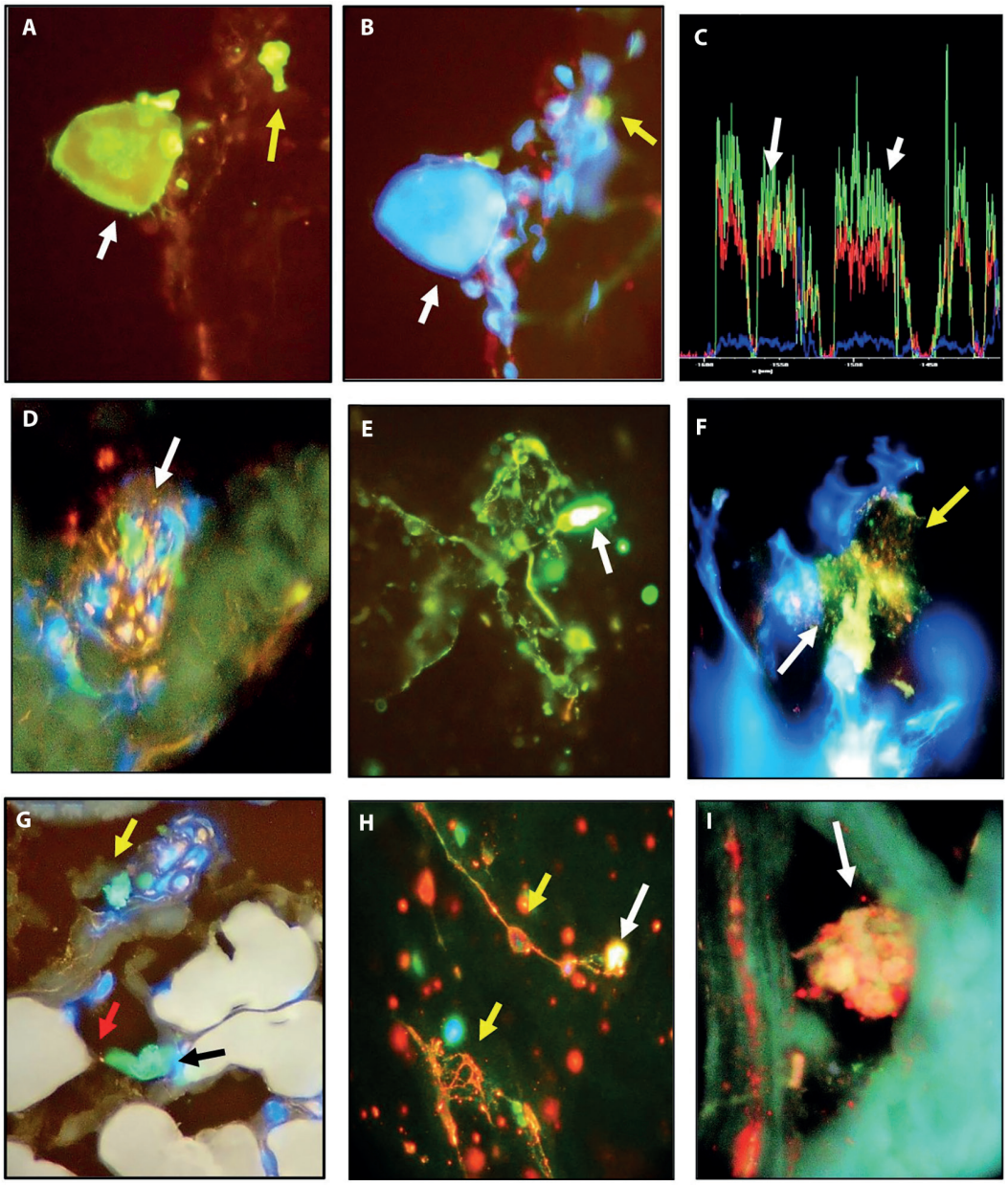

Figure 3. A through i, IIF and at 1000X. In Figures A and B, we show positive staining in SNFs. The white arrows point to large globular structures in the myelinated fibers. In A and B, we used the antibodies against FITC conjugated human complement C4 (green staining) and the antibody against desmoplakins I-II Texas red conjugated (red staining). The smaller SNFs are of unknown nature and are highlighted by yellow arrows. The nuclei of the receptors were counterstained with DAPI (blue staining). Figure 3C) Confocal microscopy (CFM) shows the perfect colocalization of the peaks detecting the antibodies (the patient antibodies in green, and desmoplakins in red; white arrows). Figures 3D to I, (also IIF). We detected reactivity against components of SNFs (white arrows). In Figure 3D, a complex SNF resembled a cauliflower with an intricate network of fine neural components; it was separated from the neighboring connective tissue by a structure lacking lamellae. In this SNF, we observed colocalization with antibodies against FITC conjugated human IgG (green staining) and the commercial antibody to MYZAP (yellowish and orange staining). These SNF was of about 350 microns in length, located at the junction of the AF connective tissue and at the paraspinous musculature. In Figures 3E and F, we also observed several SNF in which the patients autoantibodies directed to IgM FITC conjugated, perfectly colocalize with monoclonal *antibodies* against glial fibrillary acidic protein (*GFAP*) commercial antibody. In figure E, yellow arrow, and Figure F, the yellow arrow shows positive GFAP as component of this complex receptor. Figure 3 G) we show an example of two different shape SNF adjacent to a cell junction (red arrow). The receptors are shown in green, one is pointed at the black arrow, and the other with the black arrow. Figure 3F) we show examples of double SNFs that have no nuclei and were positive for anti-human FITC conjugated fibrinogen, colocalizing with the antibody against MYZAP (yellow-orange color). Figure 3H) we found net-like receptor structures (yellow arrows) using the antibodies of the patients using IgG FITC conjugated, and the commercial antibodies to GFAP. The white arrow shows a lighter receptor only reactive by GFAP. These were often seen in several areas around the IVDs; some of these SNFs resembled Meissner corpuscles. Figure 3 I, the white arrow points to a few of the SNFs that did not show the morphology of the SNFs typical of the skin.

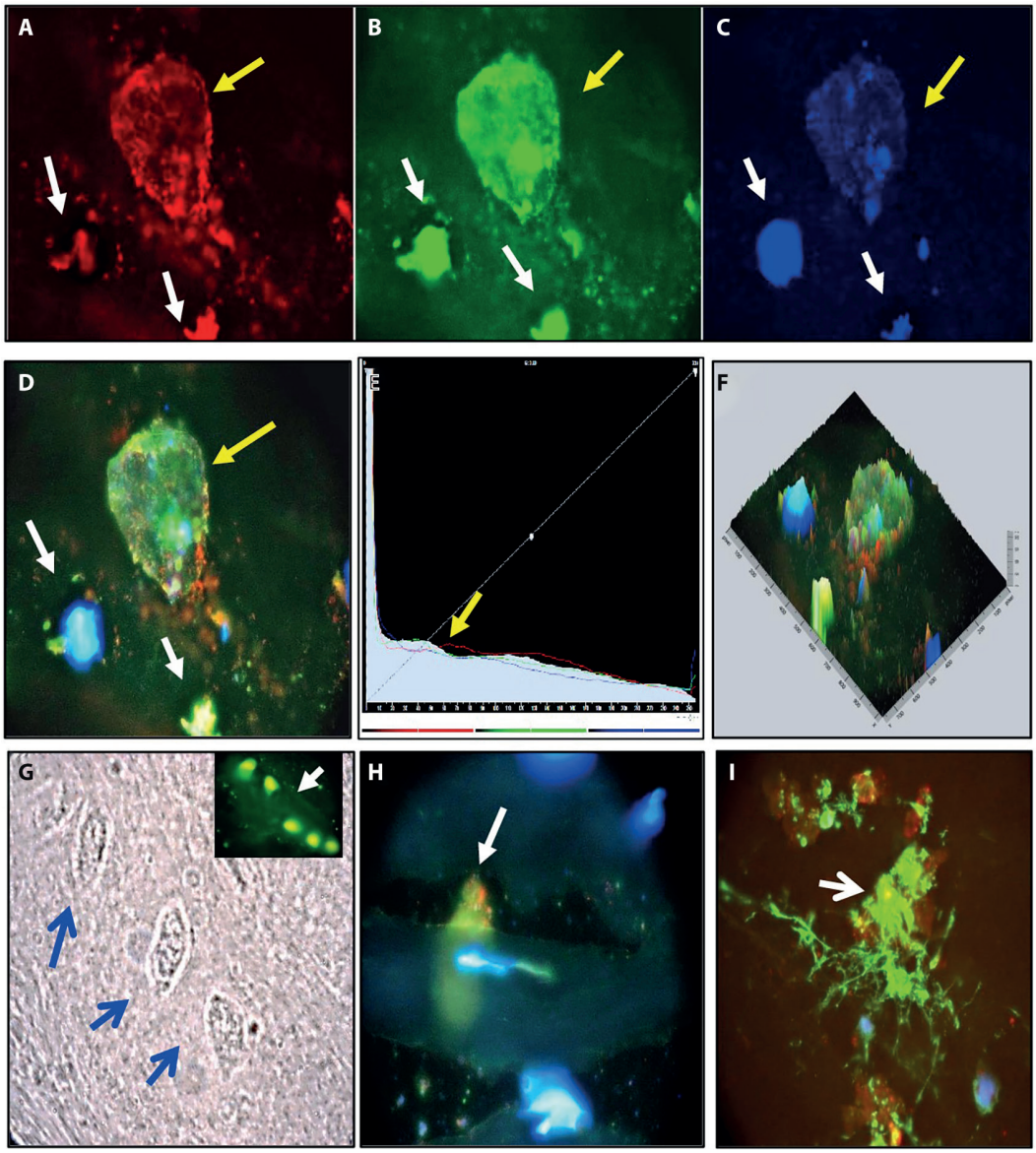

Figure 4. A-I. (All in 1000X). We observed other morphotypes of SNFs, varying considerably in size and shape. They displayed various positive areas of intricate stain inside their globular structures, differing from those documented in Figure 3. Figures 4 A, B and C show the large capsule of the larger receptors (yellow arrows), near small receptors (white arrows). The larger receptors displayed a prominent thick capsule. For Figures 4A through F, we used human FITC conjugated anti-human lambda antibodies (green staining) and a Texas red conjugated antibody against MYZAP (red staining). Both antibodies show perfect colocalization using the confocal microscopy. In Figure 4C, we demonstrate that these two types of receptors have nuclei for their positivity to DAPI (blue color). Figure 4E shows the peaks of reactivity of these antibodies perfectly colocalize (yellow arrow). Figure 4F the blue arrows shows 3D imagen demonstrating how three types of receptors being close to each other and seem to be not in the same plane suggesting a subspecialized cell signaling. Figure 4G shows a reflectance microscopy image using polarized light of three receptors of same kind of linear repetitive pattern. The IIF in Figure 4G, top right corner shows four receptors in linear pattern. Figure 4H are receptors with similar shape of Meissner receptor positive to anti human IgM antibody FITC conjugated colocalizing with the commercial antibody to p0071 Texas red conjugated. Figure 4I, using the same antibodies as in Figure 4H, we detected some clusters of SNFs with a larger receptor (white arrow) attached to a neurovascular branch of blood vessels, with at least six other SNFs of different shapes.

desmosomes, hemidesmosomes, adherent and gap junctions as well as other more complex junctions [2,7,8]. Several members of the armadillo (arm)-family of catenin proteins are part of the cell junctions in most organs of the body. These include β-catenin, plakoglobin as well as members of the p120-catenin subfamily including p120-catenin, p0071-catenin (also known as PKP4), ARVCF, δ-catenin (also known as neurojungin or neural plakophilin-related protein), and plakophilins 1-3 (frequently associated with desmosomes) [9].

Most published studies about the innervation of the IVD and adjacent ligaments in vertebrates have demonstrated that nerve fibers are found only at the periphery of the AF [10,11]. The afferent innervation of the IVD is represented

by free nerve endings and different morphotypes of SNFs, including Ruffini-like, simple lamellar corpuscles, and Pacini-like and Golgi-like corpuscles [12]. On the other hand, the paradiscal ligaments also have rich innervation.[10-13] However, most of the SNF morphotypes we identified did not correspond to the classic ones described in the skin and joints. This may be attributable, at least in part, to changes in SNFs caused by the disease itself.

An important question remains: which of the main components of SNFs are targeted by the autoantibodies of El Bagre-EPF patients? SNFs or sensory corpuscles, [14] also known collectively as end-organ structures, [14] and cutaneous end-organ complexes in the skin [16] are placed at the peripheral tip of nociceptors (as free nerve endings) or low-threshold mechanoreceptors (LTMRs) [17]. Structurally, SNFs consist of a nociceptor or LTMRs-axon close to terminal glial cells and variably arranged [15,18], with a more or less developed capsule of endoneurial-perineurial cells, all embedded in a biochemically complex extracellular matrix.[19] The proteins identified in the different components of SNFs have included structural and axoplasmic proteins, proteins for synaptic vesicles, membrane receptors for different growth factors, ion channels, intercellular adhesion proteins, and others [19, 20]. Therefore, given the complexity and variety of proteins present in SNF cells, it is very difficult to know which ones are autoantigens in El Bagre-EPF patients.

Of great interest is the concept that has been overlooked regarding communications and signals, including the neural receptors, postsynaptic communications, and other living processes that are not simply linear and, or in two planes but in multiple dimensions. This perception was indeed demonstrated that an electrostatic motif exists on the outward part of biological macromolecules as a certain structural pattern of electrostatic potentials [21]. Indeed, we have observed over and over that the antigens in El Bagre-EPF are often located in cells junctions in at least three or multidimensional planes. Therefore, as suggested by Botti SA et al. (1988), [21] we believe studying as a whole the receptors in both interfaces that are possibly linked with lipids and water. Additionally, the α/β-hydrolase fold superfamily of proteins (neural cell adhesion members) utilize their extracellular or soluble cholinesterase-like domain to attach associated partners across cell membranes, however the neuroligins can be present intracellularly [22].

Conclusion

The clinical significance of the presence of autoantigens in the sera of El Bagre-EPF patients and the possible correlation between these findings and lower back pain reported by most El Bagre-EPF patients with the systemic form remains to be clarified. We conclude that patients affected by a new variant of endemic pemphigus foliaceus in El Bagre have autoantibodies to lumbar IVDs and surrounding structures, especially SNFs. Using conformational antibodies, we were able to explore the intricate nature of these SNFs. Because these autoantibodies have multiple conformational epitopes, they thus represent an outstanding tool to be used in biotechnological and clinical applications.

References

1. Abréu-Vélez AM, Hashimoto T, Bollag WB. A unique form of endemic pemphigus in Northern Colombia. J Am Acad Dermatol. 2003;49(4):599-608. DOI: 10.1067/s0190-9622(03)00851-x. PMID: 14512903.
2. Abreu-Velez AM, Zhe J, Howard MS, Dudley SC. Cardiac autoantibodies from patients affected by a new variant of endemic pemphigus foliaceus in Colombia, South America. J Clin Immunol. 2011;31(6):985-97. DOI: 10.1007/s10875-011-9574-y. PMID: 21796504; PMCID: PMC3380437.
3. Jespersen MC, Peters B, Nielsen M, Marcatili P. BepiPred-2.0: improving sequence-based B-cell epitope prediction using conformational epitopes. Nucleic Acids Res. 2017;3;45(W1):W24-W29. DOI: 10.1093/nar/gkx346. PMID: 28472356; PMCID: PMC5570230.
4. Oteiza P, Baldwin MW. Evolution of sensory systems. Curr Opin Neurobiol. 2021; 71:52-59. DOI: 10.1016/j.conb.2021.08.005. PMID: 34600187.
5. Abréu-Vélez AM, Roselino AM, Howard MS, Reason IJ. Endemic pemphigus over a century: Part II. N Am J Med Sci. 2010;2(3):114-25. PMID: 22624125; PMCID: PMC3354423
6. Abrèu-Velez AM, Beutner EH, Montoya F, Bollag WB, Hashimoto T. Analyses of autoantigens in a new form of endemic pemphigus foliaceus in Colombia. J Am Acad Dermatol. 2003;49(4):609-14. DOI: 10.1067/s0190-9622(03)00852-1. PMID: 14512904.
7. Abreu-Velez AM, Howard MS, Yi H, Gao W, Hashimoto T, Grossniklaus HE. Neural system antigens are recognized by autoantibodies from patients affected by a new variant of endemic pemphigus foliaceus in Colombia. J Clin Immunol. 2011;31(3):356-68. DOI: 10.1007/s10875-010-9495-1. PMID: 21210298; PMCID: PMC4548263.
8. Abreu-Velez AM, Howard MS, Yi H, et al. Patients affected by a new variant of endemic pemphigus foliaceus have autoantibodies colocalizing with MYZAP, p0071, desmoplakins 1-2 and ARVCF, causing renal damage. Clin Exp Dermatol. 2018;43(6):692-702. DOI: 10.1111/ced.13566. PMID: 29768670.
9. Fang X, Ji H, Kim SW, Park JI, Vaught TG, Anastasiadis PZ, Ciesiolka M, McCrea PD. Vertebrate development requires ARVCF and p120 catenins and their interplay with RhoA and Rac. J Cell Biol. 2004 ;165(1):87-98. DOI: 10.1083 /jcb.200307109. PMID: 15067024; PMCID: PMC2172091.
10. Edgar MA. The nerve supply of the lumbar intervertebral disc. J Bone Joint Surg Br. Br.;89(9):1135-9. DOI: 10.1302 /0301-620X.89B9.18939. Erratum in: J Bone Joint Surg Br. 2008;90(4):543. PMID: 17905946.
11. Groh AMR, Fournier DE, Battié MC, Séguin CA. Innervation of the Human Intervertebral Disc: A Scoping Review. Pain Med. 2021;4;22(6):1281-1304. DOI: 10.1093/pm/pnab070. PMID: 33595648; PMCID: PMC8185559.

12. Bogduk N. The innervation of the lumbar spine. Spine. 1983; 8: 286-93. DOI: 10.1097/00007632-198304000-00009.PMID: 6226119
13. Peng B, Wu W, Hou S, Li P, Zhang C, Yang Y. The pathogenesis of discogenic low back pain. J Bone Joint Surg Br. 2005;87(1):62-7. PMID: 15686239.
14. Malinovský L. Sensory nerve formations in the skin and their classification. Microsc Res Tech. 1996;34(4):283-301. DOI: 10.1002/(SICI)1097-0029(19960701)34:4,<283::AID-JEMT2>3.0.CO;2-Q. PMID: 8807614.
15. Hastings RL, Valdez G. Origin, identity, and function of terminal Schwann cells. Trends Neurosci. 2024;47(6):432-446. DOI: 10.1016/j.tins.2024.03.007. PMID: 38664109; PMCID: PMC11168889.
16. Handler A, Ginty DD. The mechanosensory neurons of touch and their mechanisms of activation. Nat Rev Neurosci. 2021;22(9):521-537. DOI: 10.1038/s41583-021-00489-x. PMID: 34312536; PMCID: PMC8485761.
17. Zimmerman A, Bai L, Ginty DD. The gentle touch receptors of mammalian skin. Science. 2014;346(6212):950-4. DOI: 10.1126/science.1254229. PMID: 25414303; PMCID: PMC4450345.
18. Suazo I, Vega JA, García-Mesa Y, García-Piqueras J, García-Suárez O, Cobo T. The Lamellar Cells of Vertebrate Meissner and Pacinian Corpuscles: Development, Characterization, and Functions. Front Neurosci. 2022; 16:790130. DOI: 10.3389/fnins.2022.790130. PMID: 35356056; PMCID: PMC8959428.
19. Cobo R, García-Piqueras J, Cobo J, Vega JA. The Human Cutaneous Sensory Corpuscles: An Update. J Clin Med. 2021;10(2):227. DOI: 10.3390/jcm10020227. PMID: 33435193; PMCID: PMC7827880.
20. Vega JA, García-Suárez O, Montaño JA, Pardo B, Cobo JM. The Meissner and Pacinian sensory corpuscles revisited new data from the last decade. Microsc Res Tech. 2009; 72: 299-309. DOI:10.1002/jemt.20651. PMID:19012318.
21. Botti SA, Felder CE, Sussman JL, Silman I. Electrotactins: a class of adhesion proteins with conserved electrostatic and structural motifs. Protein Eng. 1998;(6):415-20. DOI: 10.1093/protein/11.6.415. PMID: 9725619.
22. Comoletti D, Trobiani L, Chatonnet A, Bourne Y, Marchot P. Comparative mapping of selected structural determinants on the extracellular domains of cholinesterase-like cell-adhesion molecules. Neuropharmacology. 2021;184:108381. DOI: 10.1016/j.neuropharm.2020.108381. PMID: 33166544.